Mechanism and Inhibition of saFabI, the Enoyl Reductase from *Staphylococcus aureus*[†]

Hua Xu,[‡] Todd J. Sullivan,[‡,⊗] Jun-ichiro Sekiguchi,[§] Teruo Kirikae,[§] Iwao Ojima,[‡] Christopher F. Stratton,[‡,○] Weimin Mao,[∥] Fernando L. Rock,[∥] M. R. K. Alley,[∥] Francis Johnson,[‡] Stephen G. Walker,[⊥] and Peter J. Tonge*[,‡]

Institute for Chemical Biology & Drug Discovery, Department of Chemistry, Stony Brook University, Stony Brook, New York 11794-3400, School of Dental Medicine, Stony Brook University, Stony Brook, New York 11794, Department of Infectious Diseases, International Medical Center of Japan, Tokyo 162-8655, Japan, and Discovery Biology, Anacor Pharmaceuticals Inc., Palo Alto, California 94303

Received January 5, 2008; Revised Manuscript Received February 5, 2008

ABSTRACT: Approximately one-third of the world's population carries *Staphylococcus aureus*. The recent emergence of extreme drug resistant strains that are resistant to the "antibiotic of last resort", vancomycin, has caused a further increase in the pressing need to discover new drugs against this organism. The *S. aureus* enoyl reductase, saFabI, is a validated target for drug discovery. To drive the development of potent and selective saFabI inhibitors, we have studied the mechanism of the enzyme and analyzed the interaction of saFabI with triclosan and two related diphenyl ether inhibitors. Results from kinetic assays reveal that saFabI is NADPH-dependent, and prefers acyl carrier protein substrates carrying fatty acids with long acyl chains. On the basis of product inhibition studies, we propose that the reaction proceeds via an ordered sequential ternary complex, with the ACP substrate binding first, followed by NADPH. The interaction of NADPH with the enzyme has been further explored by site-directed mutagenesis, and residues R40 and K41 have been shown to be involved in determining the specificity of the enzyme for NADPH compared to NADH. Finally, in preliminary inhibition studies, we have shown that triclosan, 5-ethyl-2-phenoxyphenol (EPP), and 5-chloro-2-phenoxyphenol (CPP) are all nanomolar slow-onset inhibitors of saFabI. These compounds inhibit the growth of *S. aureus* with MIC values of 0.03–0.06 μg/mL. Upon selection for resistance, three novel *safabI* mutations, A95V, I193S, and F204S, were identified. Strains containing these mutations had MIC values ~100-fold larger than that of the wild-type strain, whereas the purified mutant enzymes had K_i values 5−3000-fold larger than that of wild-type saFabI. The increase in both MIC and K_i values caused by the mutations supports the proposal that saFabI is the intracellular target for the diphenyl ether-based inhibitors.

Staphylococcus aureus is one of the most common causative agents of hospital-acquired infections (*1, 2*). It is estimated that 30% of healthy people carry *S. aureus*, usually in the anterior nares, providing a ready reservoir for future infection (*3*). *S. aureus* is able to acquire resistance to antibiotics rapidly, and penicillin-resistant strains developed after only a few months of clinical trials (*4*). After methicillin was introduced to treat penicillin-resistant *S. aureus* in 1960, methicillin-resistant *S. aureus* (MRSA) was isolated within one year (*5*). The percentage of MRSA has been increasing continuously in the past few decades. In the United States, MRSA increased from 2.4% in 1975 (*6*) to 35% in 1996 (*7*). Currently, glycopeptide antibiotics, such as vancomycin and teicoplanin, are considered to be the only antibiotics for treating MRSA infections. However, the recent emergence of clinical isolates of vancomycin-resistant *S. aureus* (VRSA) (*8, 9*) reaffirms the pressing need to continuously discover new antibiotics against this bacterium.

Fatty acid biosynthesis is divided into two types, FASI[1] and FASII, on the basis of whether the reactions are performed by a single polypeptide or by individual enzymes. The FASI pathway usually exists in vertebrates and certain bacteria, whereas the FASII pathway, as shown in Scheme 1, is usually found in plants and bacteria. The inhibition of the FASII pathway in bacteria causes the breakdown of the cell wall and the disruption of the cell membrane (*10, 11*), demonstrating its importance for bacterial survival. A number of studies suggest that the enoyl reductase (FabI), which catalyzes the final and rate-limiting step in each cycle, is a regulator of the FASII pathway and is essential for the viability of bacteria (*12*). Because of its necessity and low

[†] This work was supported in part by NIH Grants AI44639 and AI70383.

* To whom correspondence should be addressed. Telephone: (631) 632-7907. Fax: (631) 632-7960. E-mail: peter.tonge@sunysb.edu.

[‡] Department of Chemistry, Stony Brook University.

[⊗] Current address: Department of Pharmacology; Yale University School of Medicine; New Haven, CT 06511.

[§] International Medical Center of Japan.

[○] Current address: Tri-Institutional Training Program in Chemical Biology, Memorial Sloan-Kettering Cancer Center, New York, NY 10065.

[∥] Anacor Pharmaceuticals Inc.

[⊥] School of Dental Medicine, Stony Brook University.

[1] Abbreviations: FAS, fatty acid biosynthesis; ACP, acyl carrier protein; NAC, *N*-acetylcysteamine; CoA, coenzyme A; DDsaACP, dodecenoyl saACP; MIC, minimum inhibitory concentration; EPP, 5-ethyl-2-phenoxyphenol; CPP, 5-chloro-2-phenoxyphenol.

10.1021/bi800023a CCC: $40.75
Published on Web 03/13/2008

Scheme 1: Type II Fatty Acid Biosynthesis Pathway

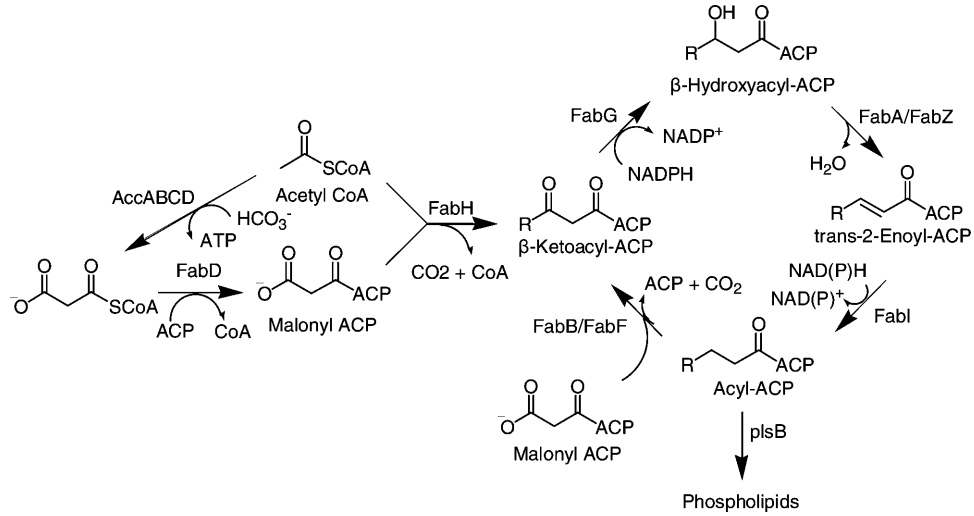

Scheme 2: Diphenyl Ether saFabI Inhibitors

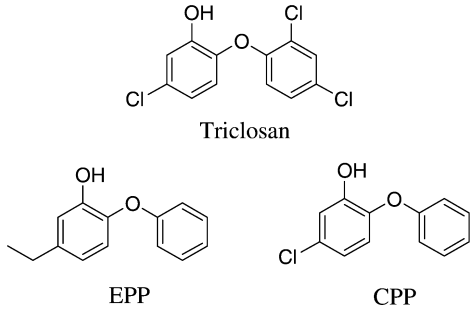

degree of sequence homology to the mammalian FASI reductase, FabI is an attractive target for novel antibiotic discovery. Isoniazid, which has been used in tuberculosis (TB) chemotherapy for decades, is now known to target InhA, the FabI homologue in *Mycobacterium tuberculosis* (*13*). A number of inhibitors against FabI have been reported recently (*14–19*). In this study, we have examined the mechanism of saFabI, as a prelude to the development of potent inhibitors of this enzyme.

Although kinetic studies on saFabI have been conducted previously, a detailed mechanistic analysis of the enzyme has so far not been reported. In addition, existing studies are based on *N*-acetylcysteamine (NAC)- or CoA-based substrates, rather than the natural acyl carrier protein (ACP) substrates (*20, 21*). In this work, we compare the kinetic properties of NAC-, CoA-, and ACP-based substrates with those of saFabI, explore the molecular basis for cofactor specificity, and also study the mechanism of the saFabI-catalyzed reaction. In addition, we have also analyzed the inhibition of saFabI by triclosan and two related diphenyl ethers, 5-ethyl-2-phenoxyphenol (EPP) and 5-chloro-2-phenoxyphenol (CPP) (Scheme 2). Triclosan is a broad-spectrum antimicrobial that is present in a wide variety of consumer products, such as toothpaste, mouthwashes, and hand soaps (*22*). It has been reported that triclosan can inhibit the growth of *S. aureus* (*23*), and this compound is recommended as a method of controlling MRSA in hospitals (*24, 25*). To extend previous studies concerning the mode of action of triclosan (*20, 21, 26, 27*), we performed selection experiments and identified several saFabI mutations that correlated with an increase in resistance to the three inhibitors. Analysis of the impact of these mutations on cell growth and enzyme inhibition strongly suggests that the diphenyl ether-based inhibitors target saFabI within the bacterium.

MATERIALS AND METHODS

Materials. *trans*-2-Dodecenoic acid was purchased from TCI. His-bind Ni^{2+}-NTA resin was obtained from Invitrogen, and centriplus units were from Millipore. The QuikChange site-directed mutagenesis kit was obtained from Stratagene. Triclosan was a gift from Ciba, whereas 5-ethyl-2-phenoxyphenol (EPP) and 5-chloro-2-phenoxyphenol (CPP) were available from a previous study (*28, 29*). All other chemical reagents were purchased from Sigma-Aldrich.

Synthesis of trans-2-Dodecenoyl-CoA and trans-2-Dodecenoyl-N-acetylcysteamine. *trans*-2-Dodecenoyl-CoA (DDCoA) was synthesized by using the mixed anhydride method as described previously (*30*). This method was also used to synthesize *trans*-2-dodecenoyl-*N*-acetylcysteamine (DDNAC) with minor modifications. Briefly, 4 mmol of *N*-acetylcysteamine was dissolved in 10 mL of anhydrous THF, and then 4 mmol of the mixed anhydride was added. After the mixture had been stirred at room temperature for 2 h, DDNAC was purified by silica gel chromatography using a 1:1 ethyl acetate/hexane mixture as the eluant. The identity of the product was confirmed by NMR spectroscopy and ESI mass spectrometry: ^{1}H NMR δ 0.880 (3H, t), 1.265 (12H, m), 1.964 (3H, s), 2.165–2.237 (2H, q), 3.090 (2H, t), 3.435–3.496 (2H, q), 6.094–6.156 (1H, m), 6.886–6.984 (1H, m); mass *m*/*z* 300.2 [$(M + H)^+$].

Expression and Purification of saFabI. The *fabI* gene from methicillin-sensitive *S. aureus* strain NCTC 8325 was amplified using the KOD DNA polymerase (Novagen) and the primers listed in Table S1 of the Supporting Information. The 0.77 kb PCR product was digested with *Nde*I and *Bam*HI and cloned into the same restriction sites in pET-16b. The sequence of the construct was confirmed by DNA sequencing (Sequetech), and the plasmid was then transformed into *Escherichia coli* strain BL21(DE3)plysS. A single colony was used to inoculate 10 mL of LB medium containing 50 μg/mL ampicillin (LB/AMP), and the culture was grown at 37 °C overnight. The cells in the starter culture were collected

by centrifugation, resuspended in fresh medium, transferred to 500 mL of LB/Amp medium, and grown at 37 °C until an optical density of 0.8 at 600 nm had been reached. Subsequently, 0.5 mM IPTG was added to induce the expression of saFabI, and the culture was shaken overnight at 25 °C. The cells were harvested and resuspended in 30 mL of His binding buffer [20 mM Tris-HCl, 500 mM NaCl, and 5 mM imidazole (pH 7.9)]. After the cells had been disrupted by being passed three times through a French pressure cell (1000 psi), the cell lysate was centrifuged at 120000*g* for 1 h, and the supernatant was loaded onto a 5 mL Ni^{2+}-NTA His-bind column, which had been preincubated with 20 mL of binding buffer. The His-bind column was washed with 40 mL of binding buffer, followed by 30 mL of wash buffer [20 mM Tris-HCl, 500 mM NaCl, and 60 mM imidazole (pH 7.9)], and saFabI was then eluted using 30 mL of elute buffer [20 mM Tris-HCl, 500 mM NaCl, and 500 mM imidazole (pH 7.9)]. SDS−PAGE was used to identify those fractions containing saFabI, and these fractions were combined and subjected to size exclusion chromatography on a G25 column using 30 mM PIPES, 150 mM NaCl, and 100 mM EDTA (pH 7.8) as the mobile phase. Fractions containing saFabI were pooled and concentrated using a Centriplus 30 apparatus.

Site-Directed Mutagenesis, Expression, and Purification of FabI Mutants. Site-directed mutagenesis was performed using the QuikChange mutagenesis kit from Stratagene using the primers listed in Table S1. The sequence of each mutant plasmid was confirmed by ABI DNA sequencing, and the expression and purification of each saFabI mutant followed the same protocol that is described above for the wild-type saFabI protein.

Cloning, Expression, and Purification of saACP. The *S. aureus acp* gene was PCR amplified from NCTC 8325 genomic DNA using the primers listed in Table S1, digested with *Nde*I and *Xho*I, and then ligated into the pET23b expression vector so that the coding region of the gene was in-frame with a C-terminal His tag. After DNA sequencing had been carried out, saACP was expressed and purified using the procedure described above for saFabI. After purification, saACP was dialyzed into 75 mM Tris-HCl and 10 mM $MgCl_2$ (pH 7.5) and the protein concentration determined using the Bradford method (*31*).

Enzymatic Preparation of Crotonyl-saACP and Dodecenoyl-saACP. Conformationally sensitive SDS−PAGE and ESI-MS revealed that saACP expressed and purified from *E. coli* was obtained primarily in the apo form. This protein was converted to the required acyl-saACP using sfp, a phosphopantetheinyl transferase from *Bacillus subtilis* (*32*). Briefly, 25 mg/L apo-saACP was incubated with 80 μM crotonyl-CoA or dodecenoyl-CoA in the presence of 1 μM sfp for 2 h at 37 °C. The reaction mixture was then loaded onto a Q-Sepharose column and eluted with a gradient consisting of buffer A [20 mM Bis-Tris (pH 7.0)] and buffer B [20 mM Bis-Tris and 800 mM NaCl (pH 7.0)]. Fractions were analyzed by SDS−PAGE, and those containing crotonyl-saACP or DDsaACP were pooled and dialyzed into 20 mM Tris-HCl (pH 7.0). The final products were characterized by ESI-MS.

Steady-State Kinetic Assays. Steady-state kinetics were determined at 25 °C in 100 mM Na_2HPO_4 buffer (pH 7.8). Initial velocities were measured after addition of 50 nM saFabI to give a final assay volume of 500 μL.

For DDsaACP, the reactions were carried out by varying the concentration of DDsaACP at several fixed concentrations of NADPH (50, 100, and 250 μM) or by varying the NADPH concentration at several fixed concentrations of DDsaACP (4.4, 8.2, and 15.0 μM). Kinetic parameters were obtained by fitting the data to eq 1 for a sequential mechanism with GraFit 4.0.

$$v = (V_{max}[A][B])/(K_{ia}K_{mb} + K_{ma}[B] + K_{mb}[A] + [A][B]) \quad (1)$$

K_{ma} and K_{mb} are the K_m values of DDsaACP and NADPH, respectively, whereas K_{ia} is the dissociation constant for DDsaACP.

For crotonyl-saACP, as well as the NAC- and CoA-based substrates, the kinetic studies employed a concentration range for one substrate ($0.3-4K_m$) at a near-saturating concentration of the second substrate. Kinetic parameters were calculated by fitting the data to the Michaelis–Menten equation (eq 2) using GraFit 4.0.

$$v = (V_{max}[S])/(K_m + [S]) \quad (2)$$

k_{cat} values were obtained by using the relationship between k_{cat} and V_{max} ($V_{max} = k_{cat}[E]$).

Product Inhibition Assays. Product inhibition studies were conducted by varying the concentration of DDsaACP at a fixed concentration of NADPH (250 μM) and at different fixed concentrations of $NADP^+$ (0, 1.4, and 2.7 mM) or by varying the concentration of NADPH at a fixed concentration of DDsaACP (20 μM) and at different fixed concentrations of $NADP^+$ (0, 0.7, and 1.4 mM).

The type of inhibition was determined using Lineweaver–Burk plot analysis. Inhibition constants for competitive, uncompetitive, and noncompetitive inhibitors were determined by globally fitting all the data points to eqs 3−5, respectively, by using GraFit 4.0.

$$v = (V_{max}[S])/[K_m(1 + [I]/K_{is}) + [S]] \quad (3)$$

$$v = (V_{max}[S])/[K_m + [S](1 + [I]/K_{ii})] \quad (4)$$

$$v = (V_{max}[S])/[K_m(1 + [I]/K_{is}) + [S](1 + [I]/K_{ii})] \quad (5)$$

The abbreviations K_{is} and K_{ii} represent the K_i slope and intercept, respectively, in the double-reciprocal plot according to the nomenclature of Cleland (*33*). Here, K_{is} and K_{ii} correspond to the dissociation constants of the inhibitor from E and ES, respectively.

Fluorescence Titration. Equilibrium fluorescence titrations were performed using a Fluorolog-3-21 fluorimeter (Spex) at 25 °C by making microliter additions of ligand to a solution containing 1 μM saFabI. In the fluorescence titration of saFabI with ACP or the diphenyl ethers, the excitation wavelength was 290 nm and the emission wavelength was 335 nm. When saFabI was titrated with NADPH, the excitation wavelength was 350 nm and the emission wavelength was 460 nm. A control experiment was performed using an identical procedure except that enzyme was omitted from the cuvette. K_d values were calculated by fitting the data to eq 6.

$$\Delta F = \Delta F_{max}\{(K_d + E + L) - [(K_d + E + L)^2 - 4K_dL]^{1/2}\}/(2E) \quad (6)$$

Selection for Resistance. Cells from the methicillin-resistant *S. aureus* strain N315 were incubated at 37 °C in

Mueller-Hinton broth (Becton-Dickinson) containing 0.02 μM triclosan, 0.08 μM EPP, or 0.08 μM CPP. After 48 h, 100 μL of each culture was plated onto Mueller-Hinton agar medium containing 0.08 μM triclosan, 0.15 μM EPP, and 0.15 μM CPP. The plates were incubated at 37 °C for 24 h. Resistant colonies were picked, and their phenotype was confirmed by regrowth on the same medium containing selective concentrations of triclosan, EPP, and CPP. The *S. aureus fabI* gene from the diphenyl ether-resistant mutants was characterized by double-strand nucleotide sequencing of PCR products amplified with *Ex-taq* polymerase (Takara Bio, Shiga, Japan) and the following primers: SafabI-F (5′-GTCATCATGGGAATCGCTAA-3′) and SafabI-R (5′-GCGTGGAATCCGCTATCTAC-3′). Sequencing reactions were performed using the SafabI-F and SafabI-R primers with the ABI PRISM BigDye Terminator Cycle Sequencing Ready Reaction Kit (Applied Biosystems, Foster City, Calif), and sequencing data were obtained using an Applied Biosystems 3100 DNA sequencer.

MIC Measurement. The MIC values were determined with the microbroth dilution assay according to the Clinical and Laboratory Standards Institute methods for antimicrobial susceptibility tests for aerobically growing bacteria (*34*).

Preincubation Inhibition Assays for Slow-Binding Inhibitors. Kinetic assays were performed essentially as described previously (*28*). Briefly, a 500 μL reaction mixture containing 50 nM saFabI, 250 μM NADPH, and various concentrations of diphenyl ether inhibitors (0−2 μM) at different fixed concentrations of $NADP^+$ (20–800 μM) was preincubated at 4 °C for 3 h. The reaction mixture was then warmed to room temperature, and the reaction was initiated by the addition of 20 μM DDsaACP. Apparent inhibition constants ($K_{i,app}$) were calculated by fitting the data to eq 7 at each concentration of $NADP^+$

$$v_i/v_0 = 1/(1 + [I]/K_{i,app}) \quad (7)$$

Subsequently, the series of $K_{i,app}$ values were fit to eq 8 to obtain K_1 and K_2, which represent the inhibition constants for inhibitor binding to $NADP^+$-bound and NADPH-bound forms of the enzyme, respectively.

$$K_{i,app} = K_2(1 + [NADP^+]/K_{mNADP})/[1 + [NADP^+]/(K_{mNADP}K_1/K_2)] \quad (8)$$

Steady-State Inhibition Studies of Diphenyl Ethers. Steady-state inhibition experiments were performed by varying the concentration of NADPH at a fixed concentration of DDsaACP (20 μM) and at different fixed concentrations of triclosan, EPP, or CPP. Reactions were initiated by the addition of the enzyme. Unless noted, the enzyme concentration was 50 nM. The data analysis was performed as described for the product inhibition assays.

RESULTS AND DISCUSSION

Expression and Purification of Wild-Type and Mutant saFabI Proteins. The protein was purified using His-tag affinity chromatography, providing homogeneously pure recombinant protein with the predicted molecular mass (~30 kDa) as determined by SDS−PAGE. As previously reported (*20*), the protein precipitated if 100 mM EDTA was omitted from the G25 buffer. In addition, we also observed that saFabI would precipitate even in 100 mM EDTA when the enzyme concentration was higher than 40 μM.

Table 1: Kinetic Parameters for the Reduction of Different Substrates with saFabI

substrate	k_{cat} (min^{-1})	K_m (μM)	k_{cat}/K_m (min^{-1} μM^{-1})
crotonyl-NAC[a]	1.5 ± 0.5	8.0 ± 0.3	0.20 ± 0.06
crotonyl-CoA[b,c]	–	–	–
crotonyl-saACP[c]	11.6 ± 1.1	11.5 ± 2.0	1.1 ± 0.2
dodecenoyl-NAC[c]	30.4 ± 1.6	23.3 ± 2.9	1.3 ± 0.2
dodocenoyl-CoA[c]	18.0 ± 0.8	24.1 ± 2.5	0.8 ± 0.1
dodecenoyl-saACP[d]	130.2 ± 9.1	4.5 ± 0.5	29.5 ± 5.0
NADH[e]	–	–	0.010 ± 0.001
NADPH[d,e]	130.2 ± 9.1	70.8 ± 6.0	1.840 ± 0.311

[a] Parameters were measured by Heath et al. (*20*). [b] No enzymatic activity was observed. [c] Reactions were carried out with 300 μM NADPH. [d] K_m and k_{cat} values were obtained by fitting data to the sequential mechanism equation. [e] Reactions were carried out with 20 μM DDsaACP.

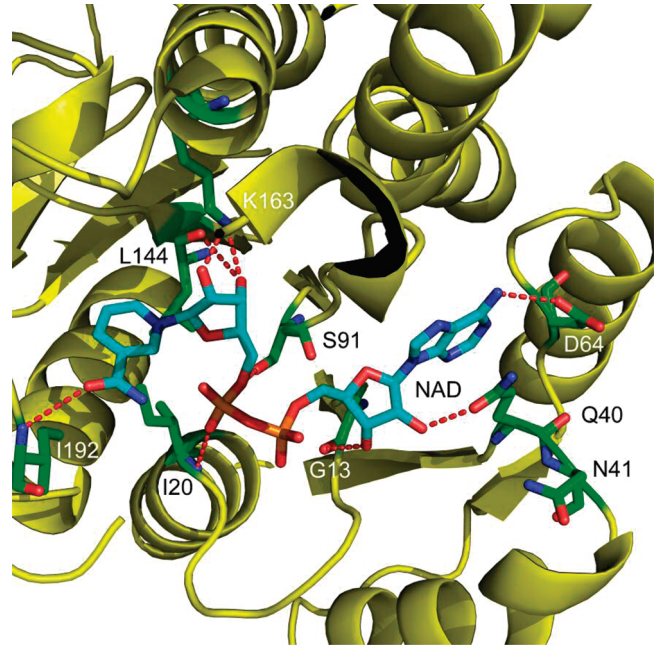

FIGURE 1: Structure of the ecFabI−NAD^+ complex. Structure of ecFabI complexed with NAD^+ (PDB entry 1DFI) showing interactions between the protein and the NAD^+ ribose. ecFabI is colored yellow, and polar interactions between the protein residues (green) and NAD^+ (cyan) are represented with red dashed lines. Q40 interacts with the 2′-hydroxyl group in the adenosine moiety of NAD^+. This figure was made using PyMol (*44*).

Preparation of ACP Substrates. saACP was purified by His-tag affinity chromatography, and only one form of ACP was observed on a 15% Tris-glycine gel, unlike the ACP (AcpM) from *M. tuberculosis* which is obtained in three forms (apo, holo, and acyl) (*35*). The ESI mass of saACP after deconvolution was 9711.6 ± 0.4, which is close to the calculated mass of apo-saACP (9707.7), suggesting that only the apo form was expressed. Subsequently, apo-saACP was converted into crotonyl-saACP or dodecenoyl-saACP (DDsaACP) by sfp, the phosphopantetheine transferase from *B. subtilis*. According to SDS−PAGE analysis, the apparent molecular mass of DDsaACP is smaller than that of apo-ACP, probably due to favorable hydrophobic interactions between the dodecenoyl acyl chain in DDsaACP and the SDS. The MW of DDsaACP was confirmed as being correct by ESI mass analysis.

Substrate Specificity. As shown in Table 1, saFabI has a 180-fold higher k_{cat}/K_m with NADPH than with NADH,

```
hiFabI   ---------------------------------------------MGFLTGKRILVTGLASNRSIAYGIAKSMKEQGAELAFTYLNDKLQPRVEEFAKEFG--SDIVLPLDVATDESIQN 73
ecFabI   ---------------------------------------------MGFLSGKRILVTGVASKLSIAYGIAQAMHREGAELAFTYQNDKLKGRVEEFAAQLG--SDIVLQCDVAEDASIDT 73
saFabI   ---------------------------------------------MLNLENKTYVIMGIANKRSIAFGVAKVLDQLGAKLVFTYRKERSRKELEKLLEQLNQPEAHLYQIDVQSDEEVIN 75
InhA     --------------------------------------------MTGLLDGKRILVSGIITDSSIAFHIARVAQEQGAQLVLTG-FDRLR-LIQRITDRLPAKAPL-LELDVQNEEHLAS 73
bsFabI   MSDSNLTNPIKAFFHDEFPEQYQEPPGLQKNMKPVPDCGEKSYKGSGKLTGRKALVTGGDSGIGRAAAIAYAREGADVAINYLPEEQPDAEEVKELIEAEGR-KAVLIPGDLSDESFCQD 119
                                                     * .:  :: *  .  . *  :*  .  .. :      :    ::.:          *:  :

hiFabI   CFAELSKRWDK---FDGFIHAIAFAPGDQLDGDYVNAATREGYRIAH-DISAYSFVAMAQAARPYLNPNAALLTLSYLGAERAIPNYNVMCLAKASLEAATRVMAADLG-KEGIRVNAIS 188
ecFabI   MFAELGKVWPK---FDGFVHSIGFAPGDQLDGDYVNAVTREGFKIAH-DISSYSFVAMAKACRSMLNPGSALLTLSYLGAERAIPNYNVMGLAKASLEANVRYMANAMG-PEGVRVNAIS 188
saFabI   GFEQIGKDVGN---IDGVYHSIAFANMEDLRGRFS-ETSREGFLLAQ-DISSYSLTIVAHEAKKLMPEGGSIVATTYLGGEFAVQNYNVMGVAKASLEANVKYLALDLG-PDNIRVNAIS 189
InhA     LAGRVTEAIGAGNKLDGVVHSIGFMPQTGMGINPFFDAPYADVSKGI-HISAYSYASMAKALLPIMNPGGSIVGMDFD-PSRAMPAYNWMTVAKSALESVNRFVAREAG-KYGVRSNLVA 190
bsFabI   LVKQSHHELGG-------LDVLALVAGKQQAVENIEDLPTEQIYKTF-EVNVFSLYWVVKAALPYLPEGASIITTTSVEGYNPSPMLLDYAATKNAIIGFTVGLGKQLA-SKGIRVNSVA 230
           .  .            .  :.:          .         .:.  :*   :.:    :  ..:::          .          :* :: .    :.   .  .:* * ::

hiFabI   AGPIRT-LAASGIKN----------FKKMLSTFEKTAALRR-TVTIEDVGN-SAAFLCSDLASGITGEIVHVDAGFSITAMGELGEE 262
ecFabI   AGPIRT-LAASGIKD----------FRKMLAHCEAVTPIRR-TVTIEDVGN-SAAFLCSDLSAGISGEVVHVDGGFSIAAMNELELK 262
saFabI   ASPIRT-LSAKGVGG----------FNTILKEIEERAPLKR-NVDQVEVGK-TAAYLLSDLSSGVTGENIHVDSGFHAIK------- 256
InhA     AGPIRT-LAMSAIVGGALGEEAGAQIQLLEEGWDQRAPIGWNMKDATPVAK-TVCALLSDWLPATTGDIIYADGGAHTQLL------ 269
bsFabI   PGPIWTPLQISGGQP--------TENIPKFGQGTPPAPLNR-AGQPVELAD-VYVFLASENSSYVTSQVYGITGGIPTA-------- 299
         ..** * *  ..                        :.:           :..      * *: .   :.:      .*
```

FIGURE 2: Sequence alignment of FabIs from *E. coli*, *S. aureus*, *H. influenzae*, *M. tuberculosis*, and *B. subtilis* created using ClustalW. The red-colored amino acids are proposed to interact with the cofactor, according to the X-ray structure of the ecFabI−NAD^+ complex.

Table 2: Effect of Mutagenesis on the Specificity of saFabI for NADH and NADPH

	k_{cat}/K_m (min^{-1} μM^{-1})	
enzyme	NADPH	NADH
wild type	1.840 ± 0.311	0.010 ± 0.001
R40Q	0.020 ± 0.001	0.053 ± 0.003
K41N	0.036 ± 0.002	0.072 ± 0.002
R40Q/K41N	0.004 ± 0.001	0.076 ± 0.005

Table 3: Selection for Resistance to the Diphenyl Ether saFabI Inhibitors

		fabI gene	
mutant derived from *S. aureus* N315	selection for mutants resistant to compound	nucleotide changes[a]	amino acid changes
N315Tr.4	triclosan	GCA → G<u>T</u>A	Ala95 → Val
N315Tr.5	triclosan	GCA → G<u>T</u>A	Ala95 → Val
N315PT01.1	EPP	GCA → G<u>T</u>A	Ala95 → Val
N315PT01.2	EPP	GCA → G<u>T</u>A	Ala95 → Val
N315PT01.3	EPP	GCA → G<u>T</u>A	Ala95 → Val
N315PT01.4	EPP	GCA → G<u>T</u>A	Ala95 → Val
N315PT52.1	CPP	ATC → A<u>G</u>C	Ile193 → Ser
N315PT52.2	CPP	TTC → T<u>C</u>C	Phe204 → Ser
N315PT52.3	CPP	TTC → T<u>C</u>C	Phe204 → Ser
N315PT52.4	CPP	TTC → T<u>C</u>C	Phe204 → Ser

[a] Mutation sites are underlined.

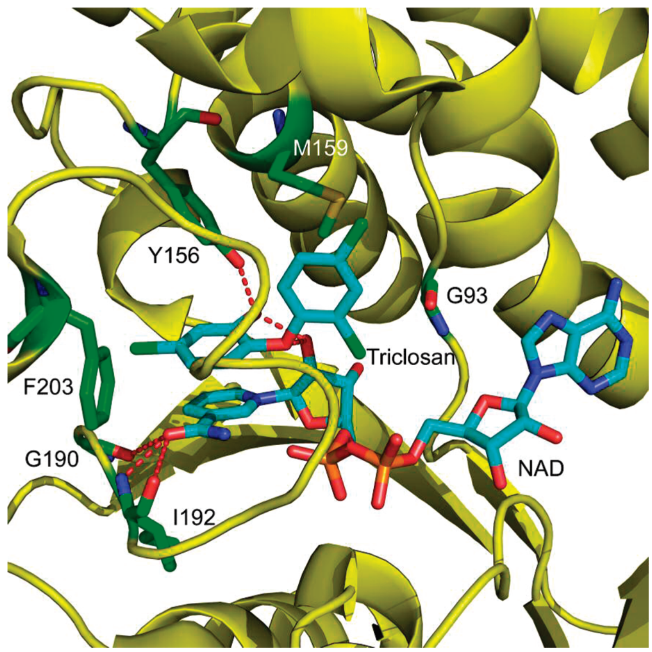

FIGURE 3: Structure of ecFabI complexed with NAD^+ and triclosan. Structure of triclosan bound to ecFabI (PDB entry 1D8A) showing the proximity of residues G93, I192, and F203 to the inhibitor binding site. The corresponding residues in saFabI were found to be mutated in the diphenyl ether-resistant *S. aureus* strains. ecFabI is colored yellow, while the polar interactions between the residues (green) in ecFabI and NAD or triclosan (cyan) are represented with red dashed lines. This figure was made using PyMol (*44*).

suggesting that saFabI is a NADPH-dependent enzyme, which is consistent with previous results when *trans*-2-octenoyl-*N*-acetylcysteamine was used as the substrate (*20*). As expected, saFabI also has a preference for ACP-linked substrates compared to those attached to NAC or CoA, indicating that saFabI is specific for its natural substrate. While we were able to detect binding of apo-saACP to saFabI (K_d = 18.2 μM) by fluorescence titration (Figure S1), no change in fluorescence could be detected upon addition of NAC or CoA, suggesting that these carriers do not bind strongly to the enzyme, in agreement with the kinetic data. In addition, the enzyme also had a preference for a long chain (C12) substrate compared to the shorter (C4) acyl group, with DDsaACP having a k_{cat}/K_m value ~30-fold larger than that for the corresponding crotonyl-ACP substrate. This effect is also observed for the NAC- or CoA-based substrates (Table 1). Interestingly, the effect of the acyl chain length on k_{cat}/K_m is primarily an effect on catalytic efficiency (k_{cat}) rather than K_m, suggesting that remote interactions between the longer acyl chain and the enzyme modulate the precise orientation of the catalytic groups in the active site. Finally, both the NAC- and CoA-based substrates suffered from some disadvantages, the NAC substrates possessing limited aque-

Table 4: Kinetic Parameters for the Reduction of DDsaACP by Wild-Type and Mutant FabIs

		NADPH		DDsaACP	
enzyme	k_{cat} (min^{-1})	K_m (μM)[a]	k_{cat}/K_m (min^{-1} μM^{-1})[a]	K_m (μM)[b]	k_{cat}/K_m (min^{-1} μM^{-1})[b]
wild type	130.2 ± 9.1	70.8 ± 6.0	1.8 ± 0.3	4.5 ± 0.5	29.5 ± 5.0
A95V	18.4 ± 0.1	269.4 ± 29.2	0.007 ± 0.001	11.4 ± 1.6	1.7 ± 0.2
I193S	−	>1000	0.13 ± 0.02	−	5.1 ± 0.4
F204S	157.3 ± 7.2	429.6 ± 45.0	0.17 ± 0.02	18.4 ± 1.3	7.8 ± 0.7

[a] Reactions were carried out with 20 μM DDsaACP. [b] Reactions were carried out with 300 μM NADPH.

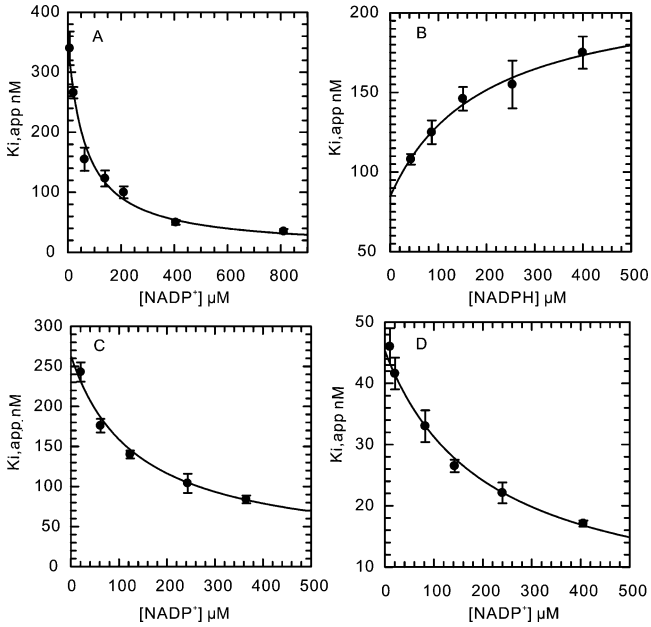

FIGURE 4: Inhibition of wild-type saFabI by the diphenyl ether inhibitors. (A) Dependence of $K_{i,app}$ on $NADP^+$ concentration for inhibition by triclosan. (B) Dependence of $K_{i,app}$ on NADPH concentration for inhibition by triclosan. (C) Dependence of $K_{i,app}$ on $NADP^+$ concentration for inhibition by EPP. (D) Dependence of $K_{i,app}$ on $NADP^+$ concentration for inhibition by CPP.

ous solubility even in the presence of 5% DMSO, whereas DDCoA exhibited substrate inhibition at high concentrations (60 μM). Substrate inhibition was not observed with DDNAC or DDsaACP, which leads to the hypothesis that the adenosine portion of CoA can bind nonproductively in the NADPH binding site.

It is interesting that saFabI is NADPH-dependent, whereas the FabI homologues from *E. coli*, *B. subtilis*, *Haemophilus influenzae*, and *M. tuberculosis* are all reported to be NADH-dependent ACP reductases (*36–38*). According to the ecFabI−NAD^+ crystal structure [Figure 1; Protein Data Bank (PDB) entry 1DFI], Q40 is very close (2.8 Å) to the 2′-hydroxyl group of the NAD^+ adenosine moiety. Sequence alignment of the FabI proteins from different organisms (Figure 2) indicates that two positively charged residues, R40 and K41, appear close to the position of Q40 in saFabI, whereas nonpolar residues (L and F) and a negatively charged residue (E) is present in the cases of the FabIs from *B. subtilis*, *H. influenzae*, and *M. tuberculosis*, respectively. Basic residues, such as R or K, in this position are expected to interact strongly with the 2′-phosphate of NADPH. To investigate the importance of R40 and K41 in the interaction of NADPH with saFabI, we constructed two single mutants, R40Q and K41N, and found that both mutants exhibit an at least 50-fold decrease in k_{cat}/K_m for NADPH, whereas k_{cat}/K_m for NADH increases by 5−7-fold (Table 2). The double mutation R40Q/K41N further decreases k_{cat}/K_m for NADPH by 10-fold, proving that both R40 and K41 are involved in interactions with the 2′-phosphate of NADPH. Since all the residues apart from Q40 which have polar interactions with NAD^+ in the ecFabI−NAD^+ crystal structure are highly conserved in saFabI, it might be expected that the cofactor specificity would be completely reversed in the saFabI double mutant. However, the NADH specificity of the double mutant remains almost the same as that of the single mutants, only 7-fold higher than that of wild-type saFabI, indicating that other factors are critical for optimal binding of NADH.

Enzymatic Mechanism of the saFabI-Catalyzed Reaction. As expected, double-reciprocal plots of the enzyme kinetic data generated intersecting lines (Figure S2A,B), which is a characteristic of a ternary complex mechanism in which NADPH transfers a hydride directly to the substrate. To determine the order of substrate binding, the effect of the product $NADP^+$ on the reaction was analyzed. Initial velocities were measured at various concentrations of DDsaACP and a fixed concentration of NADPH and at different fixed concentrations of $NADP^+$. The parallel lines in the double-reciprocal plot that were obtained (Figure S3A) suggest that $NADP^+$ is an uncompetitive inhibitor with respect to DDsaACP. However, the assays were also performed with NADPH as the varied substrate. As shown in Figure S3B, the lines intersect to the left of the *y*-axis, indicating that the $NADP^+$ is a noncompetitive inhibitor with respect to NADPH. The inhibition patterns of $NADP^+$ against the two substrates are consistent with only an ordered bi-bi mechanism, in which DDsaACP binds first, followed by NADPH.

In fluorescence titration experiments, no fluorescence change was observed when saFabI was titrated with NADPH, suggesting that NADPH does not bind to saFabI or that binding does not affect the fluorescence of the NADPH fluorophore. In contrast, a K_d value of 2.3 μM was obtained when saFabI was titrated with DDsaACP (Figure S4). These results provide further support for the proposed ordered bi-bi mechanism.

Antimicrobial Activity of the Diphenyl Ether saFabI Inhibitors. The molecular basis for the antibacterial activity of triclosan against *S. aureus* has attracted much attention. It was proposed that triclosan inhibits *S. aureus* by targeting the enoyl reductase in this organism (*20, 21, 26*), since it is known that triclosan inhibits the FabI homologue in *E. coli* (*39–41*) and that the sequence of saFabI is 43% identical to that of ecFabI. However, the observation that small-colony variants of *S. aureus* have increased resistance to triclosan suggests a more complex underlying mode of action of this antimicrobial agent (*27*).

As a first step in developing novel inhibitors against *S. aureus*, we synthesized two diphenyl ether analogues of

Table 5: Inhibition of Wild-Type and Mutant FabIs by the Diphenyl Ether Inhibitors

enzyme	compound	K_1 (nM)	K_2 (nM)	inhibition pattern	MIC against *S. aureus* N315 [μg/mL (μM)]
wild type	triclosan	4.9 ± 0.6[a]	375.1 ± 20.3[a]	UC with respect to $NADP^+$	0.03 (0.10)
		5.6 ± 0.2[b]	216.4 ± 7.5[b]	C with respect to NADPH	
	EPP[a]	8.3 ± 0.8	273.1 ± 13.2	UC with respect to $NADP^+$	0.03 (0.14)
	CPP[a]	2.0 ± 0.2	48.7 ± 1.6	UC with respect to $NADP^+$	0.06 (0.27)
A95V	triclosan[c]	8100 ± 1190	−	UC with respect to NADPH	2.80 (10)
	EPP[c]	1660 ± 50	−	UC with respect to NADPH	4.40 (20)
	CPP[c]	6150 ± 160	−	UC with respect to NADPH	8.80 (40)
I193S	triclosan[d]	35 ± 18	473 ± 196	NC with respect to NADPH	2.80 (10)
	EPP[d]	41 ± 5	783 ± 281	NC with respect to NADPH	8.80 (40)
	CPP[d]	52 ± 2	690 ± 320	NC with respect to NADPH	17.60 (80)
F204S	triclosan[c]	210 ± 20	−	UC with respect to NADPH	0.70 (2.5)
	EPP[d]	160 ± 60	300 ± 110	NC with respect to NADPH	2.20 (10)
	CPP[c]	570 ± 30	−	UC with respect to NADPH	8.80 (40)

[a] The $NADP^+$ concentration was varied. [b] The NADPH concentration was varied. [c] Uncompetitive. K_{ii} has been listed under K_1. The enzyme concentration was 200 nM. [d] Noncompetitive inhibition. K_{ii} has been listed under K_1, and K_{is} has been listed under K_2. K_{ii} and K_{is} were defined previously by Cleland (*33*).

triclosan: 5-ethyl-2-phenoxyphenol (EPP) and 5-chloro-2-phenoxyphenol (CPP). Both compounds have MIC values similar to that of triclosan against different strains of *S. aureus* (Table S2). It is very encouraging that the MIC values are similar for both methicillin-sensitive (ATCC 29213) and methicillin-resistant *S. aureus* strains (N315, Mu50), suggesting that the diphenyl ethers are orthogonal to current antibiotics. To probe the mechanism of action of the diphenyl ether inhibitors, selection experiments resulted in the identification of three novel mutations in the *fabI* gene, A95V, I193S, and F204S (Table 3), suggesting that saFabI is the intracellular target for these compounds. On the basis of the ecFabI−NAD−triclosan crystal structure (*42*), the three residues are thought to lie in the cofactor binding pocket of saFabI (Figure 3). Interestingly, the residues corresponding to A95 and F204 in ecFabI (G93 and F203, respectively) were also found to be mutated in triclosan-resistant *E. coli*. In addition, the residue corresponding to I193 in ecFabI (I192) interacts with the cofactor, as shown in Figure 3. As expected, the three saFabI mutations affected the kinetic parameters associated with NADPH more significantly than the parameters for the ACP substrate (Table 4). In particular, the k_{cat}/K_m value for NADPH decreased by 240-fold for the A95V mutant, while the k_{cat}/K_m value for DDsaACP decreased only 18-fold, confirming that the mutation has a major impact on the interaction of the cofactor with the enzyme.

To analyze further the effect of the mutations on enzyme inhibition, we quantified the interaction of the three diphenyl ether inhibitors with both wild-type and mutant saFabIs. In the case of wild-type saFabI, all three compounds were slow-onset inhibitors, binding preferentially to the enzyme−$NADP^+$ product complex. The slow step in the formation of the final enzyme–inhibitor complex is believed to result from the ordering of a flexible loop that covers the active site, which was seen for the inhibition of ecFabI by triclosan. Since the loop in ecFabI (residues 193–202) is highly conserved in saFabI, we propose that the slow step during the inhibition of saFabI by the diphenyl ethers is also caused by the loop ordering. We used the preincubation method to measure K_1 and K_2, which represent the equilibrium dissociation constants of the compounds from the E−$NADP^+$ and E−NADPH forms of the enzyme, respectively. According to the inhibition results (Figure 4A−D), the compounds are uncompetitive inhibitors of $NADP^+$ and competitive inhibitors of NADPH. K_1 is 20−40-fold smaller than K_2, suggesting that the diphenyl ethers bind preferentially to the E−$NADP^+$ form. In addition, the K_1 values correlate well with the MIC data, suggesting that saFabI is the target of this class of inhibitor. The use of eq 6 to analyze the inhibition data is based on the assumption that the inhibitors do not bind tightly to the free enzyme. In agreement with this assumption, fluorescence titrations of saFabI with the three inhibitors (Figure S5A−C) gave K_d values between 50 and 200 μM, at least 200-fold higher than either K_1 or K_2.

In contrast to the wild-type enzyme, the diphenyl ether compounds are classical reversible inhibitors of the saFabI mutant enzymes (Figures S6−S8). Triclosan, CPP, and EPP are uncompetitive or noncompetitive inhibitors of the mutant saFabIs with respect to NADPH, with K_i values 5−3000-fold higher than for the wild-type enzyme. This increase in K_i correlates with the increase in the MIC values observed for the *S. aureus* strains harboring the *safabI* mutations (Table 5). This further substantiates the hypothesis that saFabI is the target of diphenyl ethers within this bacterium. Interestingly, for the mutant I193S, K_i values of triclosan, EPP, and CPP increase by only 5−25-fold, but the MICs increase by more than 60-fold. This suggests that additional mechanisms of resistance are operative, such as the overexpression of the mutant saFabI as reported by Fan et al. (*26*). We also observed that the frequency with which each mutation occurred also correlated with the effect of that mutation on enzyme inhibition. Thus, A95V, the most frequent mutation in the resistant strains, had the greatest impact on inhibition of saFabI by the diphenyl ether inhibitors.

Finally, we also analyzed the ability of the three compounds to inhibit the growth of *Enterococcus faecalis.* This organism contains both a FabI enoyl reductase and a FabK homologue that is not sensitive to triclosan (*43*). In Table S3, it can be seen that the three diphenyl ethers have MIC values against *E. faecalis* that are ~1000-fold higher than those for *S. aureus*, again supporting the contention that the antibacterial action of these compounds is directed against FabI.

CONCLUSION

In summary, we have studied the mechanism of the reaction catalyzed by saFabI using substrates based on the natural ACP carrier molecule. From the results of the kinetic assays, we propose that the binding of substrates in the ternary complex mechanism is ordered, with DDsaACP binding first followed by NADPH. Two residues, R40 and K41, are shown to be critical for cofactor specificity. In addition, we investigated the mechanism of action of three diphenyl ether-based saFabI inhibitors. All three compounds are slow-onset inhibitors of saFabI in vitro, binding preferentially to the E−$NADP^+$ product complex with K_1 values of 2–8 nM. These compounds have potent antibacterial activity, with MIC values against *S. aureus* of 0.03–0.06 μg/mL. Selection experiments led to the identification of three mutations in the *safabI* gene, A95V, I193S, and F204S, which correlate with resistance to the diphenyl ethers and cause a significant reduction in the affinity of the inhibitors for the enzyme. These experiments confirm the hypothesis that the diphenyl ether-based inhibitors target saFabI in live cells and substantiate the view that saFabI is a novel target for antibacterial drug discovery.

ACKNOWLEDGMENT

We are grateful to Dr. Michael Burkart (University of California at San Diego, La Jolla, CA) for providing the sfp plasmid.

SUPPORTING INFORMATION AVAILABLE

Double-reciprocal plots for the kinetic and inhibition studies and the MIC data for the diphenyl ethers against the *S. aureus* mutant strains and *E. faecalis*. This material is available free of charge via the Internet at http://pubs.acs.org.

REFERENCES

1. Diekema, D. J., Pfaller, M. A., Schmitz, F. J., Smayevsky, J., Bell, J., Jones, R. N., and Beach, M. (2001) Survey of infections due to *Staphylococcus* species: Frequency of occurrence and antimicrobial susceptibility of isolates collected in the United States, Canada, Latin America, Europe, and the Western Pacific region for the SENTRY Antimicrobial Surveillance Program, 1997–1999. *Clin. Infect. Dis. 32* (Suppl. 2), S114–S132.
2. Pfaller, M. A., Jones, R. N., Doern, G. V., Sader, H. S., Kugler, K. C., and Beach, M. L. (1999) Survey of blood stream infections attributable to Gram-positive cocci: Frequency of occurrence and antimicrobial susceptibility of isolates collected in 1997 in the United States, Canada, and Latin America from the SENTRY Antimicrobial Surveillance Program. SENTRY Participants Group. *Diagn. Microbiol. Infect. Dis. 33*, 283–297.
3. Peacock, S. J., de Silva, I., and Lowy, F. D. (2001) What determines nasal carriage of *Staphylococcus aureus*? *Trends Microbiol. 9*, 605–610.
4. Bradley, S. F. (1992) Methicillin-resistant *Staphylococcus aureus* infection. *Clin. Geriatr. Med. 8*, 853–868.
5. Barber, M. (1961) Methicillin-resistant staphylococci. *J. Clin. Pathol. 14*, 385–393.
6. Panlilio, A. L., Culver, D. H., Gaynes, R. P., Banerjee, S., Henderson, T. S., Tolson, J. S., and Martone, W. J. (1992) Methicillin-resistant *Staphylococcus aureus* in U.S. hospitals, 1975–1991. *Infect. Control Hosp. Epidemiol. 13*, 582–586.
7. Gaynes, R., and Culver, D. (1997)Nosocomial methicillin-resistant *Staphylococcus aureus* (MRSA) in the United States, 1975−1996. National Nosocomial Infection Surveillance (NNIS) System. Annual Meeting of the Infectious Disease Society of America (IDSA), San Francisco.
8. From the Centers for Disease Control and Prevention (2002) Vancomycin resistant *Staphylococcus aureus*—Pennsylvania, 2002, in *Journal of the American Medical Association*, p 2116.
9. Hiramatsu, K., Hanaki, H., Ino, T., Yabuta, K., Oguri, T., and Tenover, F. C. (1997) Methicillin-resistant *Staphylococcus aureus* clinical strain with reduced vancomycin susceptibility. *J. Antimicrob. Chemother. 40*, 135–136.
10. Egan, A. F., and Russell, R. R. (1973) Conditional mutations affecting the cell envelope of *Escherichia coli* K-12. *Genet. Res. 21*, 139–152.
11. Turnowsky, F., Fuchs, K., Jeschek, C., and Hogenauer, G. (1989) envM genes of *Salmonella typhimurium* and *Escherichia coli*. *J. Bacteriol. 171*, 6555–6565.
12. Heath, R. J., and Rock, C. O. (1995) Enoyl-acyl carrier protein reductase (fabI) plays a determinant role in completing cycles of fatty acid elongation in *Escherichia coli*. *J. Biol. Chem. 270*, 26538–26542.
13. Rawat, R., Whitty, A., and Tonge, P. J. (2003) The isoniazid-NAD adduct is a slow, tight-binding inhibitor of InhA, the *Mycobacterium tuberculosis* enoyl reductase: Adduct affinity and drug resistance. *Proc. Natl. Acad. Sci. U.S.A. 100*, 13881–13886.
14. Baldock, C., Rafferty, J. B., Sedelnikova, S. E., Baker, P. J., Stuitje, A. R., Slabas, A. R., Hawkes, T. R., and Rice, D. W. (1996) A mechanism of drug action revealed by structural studies of enoyl reductase. *Science 274*, 2107–2110.
15. Karlowsky, J. A., Laing, N. M., Baudry, T., Kaplan, N., Vaughan, D., Hoban, D. J., and Zhanel, G. G. (2007) In vitro activity of API-1252, a novel FabI inhibitor, against clinical isolates of *Staphylococcus aureus* and *Staphylococcus epidermidis*. *Antimicrob. Agents Chemother. 51*, 1580–1581.
16. Kitagawa, H., Kumura, K., Takahata, S., Iida, M., and Atsumi, K. (2007) 4-Pyridone derivatives as new inhibitors of bacterial enoyl-ACP reductase FabI. *Bioorg. Med. Chem. 15*, 1106–1116.
17. Ling, L. L., Xian, J., Ali, S., Geng, B., Fan, J., Mills, D. M., Arvanites, A. C., Orgueira, H., Ashwell, M. A., Carmel, G., Xiang, Y., and Moir, D. T. (2004) Identification and characterization of inhibitors of bacterial enoyl-acyl carrier protein reductase. *Antimicrob. Agents Chemother. 48*, 1541–1547.
18. Payne, D. J., Miller, W. H., Berry, V., Brosky, J., Burgess, W. J., Chen, E., DeWolf, W. E., Jr., Fosberry, A. P., Greenwood, R., Head, M. S., Heerding, D. A., Janson, C. A., Jaworski, D. D., Keller, P. M., Manley, P. J., Moore, T. D., Newlander, K. A., Pearson, S., Polizzi, B. J., Qiu, X., Rittenhouse, S. F., Slater-Radosti, C., Salyers, K. L., Seefeld, M. A., Smyth, M. G., Takata, D. T., Uzinskas, I. N., Vaidya, K., Wallis, N. G., Winram, S. B., Yuan, C. C., and Huffman, W. F. (2002) Discovery of a novel and potent class of FabI-directed antibacterial agents. *Antimicrob. Agents Chemother. 46*, 3118–3124.
19. Zhang, Y. M., and Rock, C. O. (2004) Evaluation of epigallocatechin gallate and related plant polyphenols as inhibitors of the FabG and FabI reductases of bacterial type II fatty-acid synthase. *J. Biol. Chem. 279*, 30994–31001.
20. Heath, R. J., Li, J., Roland, G. E., and Rock, C. O. (2000) Inhibition of the *Staphylococcus aureus* NADPH-dependent enoyl-acyl carrier protein reductase by triclosan and hexachlorophene. *J. Biol. Chem. 275*, 4654–4659.
21. Slater-Radosti, C., Van Aller, G., Greenwood, R., Nicholas, R., Keller, P. M., DeWolf, W. E., Jr., Fan, F., Payne, D. J., and Jaworski, D. D. (2001) Biochemical and genetic characterization of the action of triclosan on *Staphylococcus aureus*. *J. Antimicrob. Chemother. 48*, 1–6.
22. Russell, A. D. (2004) Whither triclosan? *J. Antimicrob. Chemother. 53*, 693–695.
23. Regos, J., Zak, O., Solf, R., Vischer, W. A., and Weirich, E. G. (1979) Antimicrobial spectrum of triclosan, a broad-spectrum antimicrobial agent for topical application. II. Comparison with some other antimicrobial agents. *Dermatologica 158*, 72–79.
24. Ayliffe, G. A., Buckles, A., Casewell, M. W., Cookson, B. D., Cox, R. A., Duckworth, G. J., Griffiths-Jones, A., Heathcock, R., Humphreys, H., Keane, C. T., Marples, R. R., Shanson, D. C., Slack, R., and Tebbs, E. (1998) Revised guidelines for the control of methicillin-resistant *Staphylococcus aureus* infection in hospitals. British Society for Antimicrobial Chemotherapy, Hospital Infection Society and the Infection Control Nurses Association. *J. Hosp. Infect. 39*, 253–290.
25. Bamber, A. I., and Neal, T. J. (1999) An assessment of triclosan susceptibility in methicillin-resistant and methicillin-sensitive *Staphylococcus aureus*. *J. Hosp. Infect. 41*, 107–109.

26. Fan, F., Yan, K., Wallis, N. G., Reed, S., Moore, T. D., Rittenhouse, S. F., DeWolf, W. E., Jr., Huang, J., McDevitt, D., Miller, W. H., Seefeld, M. A., Newlander, K. A., Jakas, D. R., Head, M. S., and Payne, D. J. (2002) Defining and combating the mechanisms of triclosan resistance in clinical isolates of *Staphylococcus aureus*. *Antimicrob. Agents Chemother. 46*, 3343–3347.
27. Seaman, P. F., Ochs, D., and Day, M. J. (2007) Small-colony variants: A novel mechanism for triclosan resistance in methicillin-resistant *Staphylococcus aureus*. *J. Antimicrob. Chemother. 59*, 43–50.
28. Sivaraman, S., Sullivan, T. J., Johnson, F., Novichenok, P., Cui, G., Simmerling, C., and Tonge, P. J. (2004) Inhibition of the bacterial enoyl reductase FabI by triclosan: A structure-reactivity analysis of FabI inhibition by triclosan analogues. *J. Med. Chem. 47*, 509–518.
29. Sullivan, T. J., Truglio, J. J., Boyne, M. E., Novichenok, P., Zhang, X., Stratton, C. F., Li, H. J., Kaur, T., Amin, A., Johnson, F., Slayden, R. A., Kisker, C., and Tonge, P. J. (2006) High affinity InhA inhibitors with activity against drug-resistant strains of *Mycobacterium tuberculosis*. *ACS Chem. Biol. 1*, 43–53.
30. Parikh, S., Moynihan, D. P., Xiao, G., and Tonge, P. J. (1999) Roles of tyrosine 158 and lysine 165 in the catalytic mechanism of InhA, the enoyl-ACP reductase from *Mycobacterium tuberculosis*. *Biochemistry 38*, 13623–13634.
31. Bradford, M. M. (1976) A rapid and sensitive method for the quantitation of microgram quantities of protein utilizing the principle of protein-dye binding. *Anal. Biochem. 72*, 248–254.
32. Quadri, L. E., Weinreb, P. H., Lei, M., Nakano, M. M., Zuber, P., and Walsh, C. T. (1998) Characterization of Sfp, a *Bacillus subtilis* phosphopantetheinyl transferase for peptidyl carrier protein domains in peptide synthetases. *Biochemistry 37*, 1585–1595.
33. Cleland, W. W. (1979) Statistical analysis of enzyme kinetic data. *Methods Enzymol. 63*, 103–138.
34. CLSI (2006) *Methods for Dilution Antimicrobial Susceptibility Tests for Bacteria That Grow Aerobically*, 6th ed., Approved Standard M7-A6, Clinical and Laboratory Standards Institute, Wayne, PA.
35. Schaeffer, M. L., Agnihotri, G., Kallender, H., Brennan, P. J., and Lonsdale, J. T. (2001) Expression, purification, and characterization of the *Mycobacterium tuberculosis* acyl carrier protein, AcpM. *Biochim. Biophys. Acta 1532*, 67–78.
36. Bergler, H., Wallner, P., Ebeling, A., Leitinger, B., Fuchsbichler, S., Aschauer, H., Kollenz, G., Hogenauer, G., and Turnowsky, F. (1994) Protein EnvM is the NADH-dependent enoyl-ACP reductase (FabI) of *Escherichia coli*. *J. Biol. Chem. 269*, 5493–5496.
37. Heath, R. J., Su, N., Murphy, C. K., and Rock, C. O. (2000) The enoyl-[acyl-carrier-protein] reductases FabI and FabL from *Bacillus subtilis*. *J. Biol. Chem. 275*, 40128–40133.
38. Marcinkeviciene, J., Jiang, W., Kopcho, L. M., Locke, G., Luo, Y., and Copeland, R. A. (2001) Enoyl-ACP reductase (FabI) of *Haemophilus influenzae*: Steady-state kinetic mechanism and inhibition by triclosan and hexachlorophene. *Arch. Biochem. Biophys. 390*, 101–108.
39. Heath, R. J., Rubin, J. R., Holland, D. R., Zhang, E., Snow, M. E., and Rock, C. O. (1999) Mechanism of triclosan inhibition of bacterial fatty acid synthesis. *J. Biol. Chem. 274*, 11110–11114.
40. Heath, R. J., Yu, Y. T., Shapiro, M. A., Olson, E., and Rock, C. O. (1998) Broad spectrum antimicrobial biocides target the FabI component of fatty acid synthesis. *J. Biol. Chem. 273*, 30316–30320.
41. McMurry, L. M., Oethinger, M., and Levy, S. B. (1998) Triclosan targets lipid synthesis. *Nature 394*, 531–532.
42. Levy, C. W., Roujeinikova, A., Sedelnikova, S., Baker, P. J., Stuitje, A. R., Slabas, A. R., Rice, D. W., and Rafferty, J. B. (1999) Molecular basis of triclosan activity. *Nature 398*, 383–384.
43. Heath, R. J., and Rock, C. O. (2000) A triclosan-resistant bacterial enzyme. *Nature 406*, 145–146.
44. Delano, W. L. (2002) *The PyMOL Molecular Graphics System*, DeLano Scientific LLC, San Carlos, CA.

BI800023A